Japanese Journal of Applied Physics

The Japan Society of Applied Physics

Enhancement-Mode Metal Organic Chemical Vapor Deposition-Grown ZnO Thin-Film Transistors on Glass Substrates Using N_2O Plasma Treatment

To cite this article: Kariyadan Remashan *et al* 2010 *Jpn. J. Appl. Phys.* **49** 04DF20

View the article online for updates and enhancements.

Related content

- Improved Characteristics of Metal Organic Chemical Vapor Deposition-Grown ZnO Thin-Film Transistors by Controlling VI/II Ratio of ZnO Film Growth and Using a Modified Thin-Film Transistor Layer Structure
Kariyadan Remashan, Yong-Seok Choi, Seong-Ju Park et al.
- The Role of High- TiHfO Gate Dielectric in Sputtered ZnO Thin-Film Transistors
Nai-Chao Su, Shui-Jinn Wang, Chin-Chuan Huang et al.
- Low-Operating-Voltage Solution-Processed InZnO Thin-Film Transistors Using High-*k* $SrTa_2O_6$
Li Lu, Yuta Miura, Takashi Nishida et al.

Recent citations

- Improved Characteristics of Metal Organic Chemical Vapor Deposition-Grown ZnO Thin-Film Transistors by Controlling VI/II Ratio of ZnO Film Growth and Using a Modified Thin-Film Transistor Layer Structure
Kariyadan Remashan *et al*

This content was downloaded from IP address 115.145.196.110 on 12/12/2017 at 01:34

Enhancement-Mode Metal Organic Chemical Vapor Deposition-Grown ZnO Thin-Film Transistors on Glass Substrates Using N_2O Plasma Treatment

Kariyadan Remashan, Yong-Seok Choi[1], Se-Koo Kang[2], Jeong-Woon Bae[2], Geun-Young Yeom[2], Seong-Ju Park[1], and Jae-Hyung Jang*

Department of Information and Communications and Department of Nanobio Materials and Electronics, Gwangju Institute of Science and Technology, Gwangju 500-712, Korea
[1]*Department of Materials Science and Engineering, Gwangju Institute of Science and Technology, Gwangju 500-712, Korea*
[2]*Department of Advanced Materials Science and Engineering, Sungkyunkwan University, Suwon, Gyeonggi-do 440-746, Korea*

Received October 5, 2009; revised November 3, 2009; accepted November 9, 2009; published online April 20, 2010

Thin-film transistors (TFTs) were fabricated on a glass substrate with a metal organic chemical vapor deposition (MOCVD)-grown undoped zinc oxide (ZnO) film as a channel layer and plasma-enhanced chemical vapor deposition (PECVD)-grown silicon nitride as a gate dielectric. The as-fabricated ZnO TFTs exhibited depletion-type device characteristics with a drain current of about 24 μA at zero gate voltage, a turn-on voltage (V_{on}) of −24 V, and a threshold voltage (V_T) of −4 V. The field-effect mobility, subthreshold slope, off-current, and on/off current ratio of the as-fabricated TFTs were 5 $cm^2 V^{-1} s^{-1}$, 4.70 V/decade, 0.6 nA, and 10^6, respectively. The postfabrication N_2O plasma treatment on the as-fabricated ZnO TFTs changed their device operation to enhancement-mode, and these N_2O-treated ZnO TFTs exhibited a drain current of only 15 pA at zero gate voltage, a V_{on} of −1.5 V, and a V_T of 11 V. Compared with the as-fabricated ZnO TFTs, the off-current was about 3 orders of magnitude lower, the subthreshold slope was nearly 7 times lower, and the on/off current ratio was 2 orders of magnitude higher for the N_2O-plasma-treated ZnO TFTs. X-ray phtotoelectron spectroscopy analysis showed that the N_2O-plasma-treated ZnO films had fewer oxygen vacancies than the as-grown films. The enhancement-mode device behavior as well as the improved performance of the N_2O-treated ZnO TFTs can be attributed to the reduced number of oxygen vacancies in the channel region. © 2010 The Japan Society of Applied Physics

DOI: 10.1143/JJAP.49.04DF20

1. Introduction

Thin-film transistors (TFTs) are the building blocks of flat-panel displays based on liquid crystals and organic light-emitting diodes. At present, TFTs used in displays employ either amorphous silicon (a-Si) or polycrystalline silicon (poly-Si) as their active channel layer. In comparison with these materials, zinc oxide (ZnO) possesses attractive characteristics[1] such as a wide band gap (~3.3 eV at 300 K), high optical transparency (above 80%), low processing temperature, and higher carrier mobility, and thus there has been active research on TFTs employing a ZnO film as the channel layer.[2–24] The available experimental data on ZnO TFTs indicates their potential use in the field of displays as well as for realizing transparent and flexible electronics. Various growth methods have been employed to realize ZnO films for use as the active channel of ZnO TFTs, including molecular beam epitaxy,[2] sputtering,[3–10] pulsed laser deposition,[11–15] atomic layer deposition,[16–21] and metal organic chemical vapor deposition (MOCVD).[22–24] In principle, MOCVD offers the advantages of good reproducibility from run to run and high-quality film with better thickness uniformity.[25] In addition to these merits, it may also be possible to use MOCVD to realize TFTs employing ZnO-based heterostructures similar to high-electron-mobility transistors. Until now, research on TFTs that employ an MOCVD-grown ZnO film as the channel layer has been limited.[22–24] The MOCVD-grown ZnO TFTs reported by Jo *et al.*[22] exhibited depletion-type device characteristics with a considerable drain current of about 0.4 mA at zero gate voltage, indicating a high concentration of electrons in the ZnO channel layer. The threshold voltage (V_T) and turn-on voltage (V_{on}) of these TFTs were −5 V and <−30 V, respectively. Here, V_{on} is defined as the gate voltage at which the drain current begins to rise in a transfer curve. The MOCVD ZnO TFTs reported by Zhu *et al.*[23] too were depletion-type devices with a drain current of as much as 0.1 mA at zero gate voltage, a V_T of −29.6 V, and a V_{on} of −40 V. But, enhancement-mode ZnO TFTs are preferable to their depletion-mode counterparts because the circuit design is easier with enhancement-mode devices and also power dissipation can be minimized.[5] Therefore, realizing enhancement-mode MOCVD ZnO TFTs is of importance. Furthermore, ZnO films with lower electron concentrations are essential for realizing MgZnO/ZnO-heterostructure-based TFTs similar to high-electron-mobility transistors. Recently, Jo *et al.*[24] reported enhancement-mode MOCVD ZnO TFTs by employing a technique involving process interruptions during the ZnO film growth, and these devices exhibited a V_{on} of −4 V, a V_T of 5 V, and a drain current of 0.4 μA at zero gate voltage. Here, we perform a postfabrication N_2O plasma treatment on MOCVD ZnO TFTs to obtain enhancement-mode operating devices as well as to achieve better TFT device parameters, including off-current. For display applications, the off-current of TFTs should be as low as possible to ensure proper functioning.[26,27] While a glass substrate and plasma-deposited gate dielectric are employed in the present work for TFT fabrication, Si substrates with a thermally grown gate dielectric were employed in the work reported by Jo *et al.*[24] Furthermore, the maximum process temperature employed in this work is 350 °C whereas it was 450 °C in ref. 24. Thus, our device fabrication process is more compatible with the TFT technology used in industry.

In this paper, we report the fabrication and characteristics of ZnO TFTs that employ an MOCVD- grown ZnO film as the active channel layer and plasma-enhanced chemical vapor deposition (PECVD)-prepared silicon nitride as the gate dielectric. These ZnO TFTs were fabricated on glass substrates and have a bottom-gated structure. The effect of postfabrication N_2O plasma treatment on the electrical characteristics of the ZnO TFTs was studied. The structural and optical properties of both the as-grown and N_2O-plasma-treated ZnO films are reported. The results

*E-mail address: jjang@gist.ac.kr

 © 2010 The Japan Society of Applied Physics

of X-ray photoelectron spectroscopy (XPS) surface analysis of the as-grown and N_2O-treated ZnO samples are also presented.

2. Experimental Procedure

2.1 Fabrication of bottom-gated ZnO TFTs

Corning 1737 glass plates coated with 200-nm-thick indium tin oxide (ITO) were used as starting substrates (Delta Technologies) for fabricating bottom-gated ZnO TFTs. The ITO acts as the gate electrode for the TFTs and it had a sheet resistance of 4–8 Ω/□. The substrates were ultrasonically cleaned with acetone, methanol, and deionized water. Firstly, the ITO gate electrodes were defined by standard photolithography and wet etching using LCE-12k (Cyantek ITO Etchant) solution at 45 °C. Following this, about 90-nm-thick silicon nitride gate dielectric was deposited by PECVD using SiH_4, NH_3, and N_2 gases (Oxford Instruments Plasmalab System 100). The process parameters used for the silicon nitride deposition were as follows: flow rates of $SiH_4/NH_3/N_2 = 20/40/600$ sccm, temperature is 300 °C, pressure is 650 mTorr, and power is 30 W.

Next, ZnO film was grown using a commercially available MOCVD vertical reactor (Sysnex ZEUS230G). Diethylzinc (DEZn) and O_2 were employed as the sources of zinc and oxygen, respectively. The DEZn source was maintained at a temperature of 0 °C and Ar was used as its carrier gas. The DEZn and O_2 were separately introduced into the reactor and the mixing of these two sources took place only 1 cm before reaching the substrate. For the ZnO film growth, the flow rates of DEZn and oxygen were 6.7 and 3.3×10^5 μmol/min, respectively. The reactor pressure was maintained at 50 Torr and the growth temperature was set to 350 °C. Under the aforementioned conditions, the growth rate of the ZnO film was about 30 Å/min.

The ZnO film was subsequently patterned by conventional photolithography and etching using $HCl : HNO_3 : H_2O$ (4 : 1 : 200) solution at room temperature. The source/drain electrodes of TFTs were next realized by the electron-beam evaporation of Ti/Pt/Au (20/30/150 nm) metal layers and the lift-off process. The TFT fabrication process was completed with the opening of vias to access the bottom ITO gate electrode, and this was done by standard photolithography and plasma etching of the silicon nitride film with CF_4/O_2 gas mixtures. No surface passivation was employed on the ZnO TFTs. The schematic cross-section and the scanning electron microscopy (SEM) top view of a fabricated ZnO TFT are shown in Figs. 1(a) and 1(b), respectively. The electrical characteristics of the ZnO TFTs, having a channel length (L) of 20 μm and a width (W) of 200 μm, were measured using a semiconductor parameter analyzer (HP-4155A).

2.2 Characterization of silicon nitride and ZnO films

In order to obtain the dielectric constant of the silicon nitride gate dielectric film, metal–insulator–metal capacitors were fabricated separately on ITO-coated Corning glass substrates using ITO and Ti/Pt/Au as electrodes and silicon nitride as an insulator. The dielectric constant estimated from the 1 MHz capacitance-voltage characteristics of the capacitors was 6.0. An XPS analysis was carried out to determine the atomic concentration ratio of N/Si in the silicon nitride film, which was found to be 1.45. The measured refractive index of the silicon nitride film was 1.8.

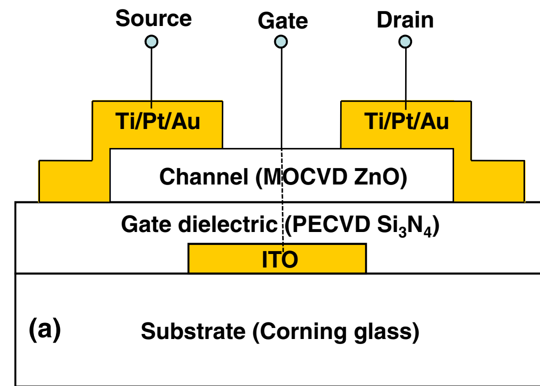

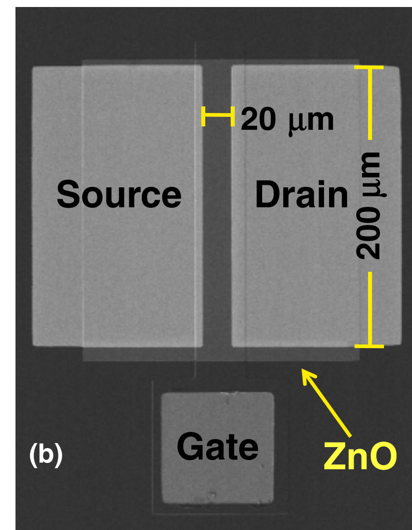

Fig. 1. (Color online) (a) Schematic cross-section and (b) SEM top view of the fabricated ZnO TFTs.

The thickness of the ZnO film measured using a surface profiler (Tencor Alpha-Step 500) was 1600 Å. The structural properties of the ZnO films were evaluated using X-ray diffraction (XRD; Rigaku D/MAX-2500) with a Cu $K\alpha$ X-ray source. A scanning electron microscope (Hitachi S-4700) was used to observe the surface morphology and cross-sectional structure of ZnO films. Photoluminescence (PL) measurements were performed at room temperature using a Ti-sapphire laser (350 nm) with an excitation power of 50 mW. XPS measurements on the ZnO samples were carried out using a MultiLab 2000 X-ray photoelectron spectrometer (Thermo Electron) with a Mg $K\alpha$ X-ray source ($h\nu = 1253.60$ eV).

2.3 N_2O plasma treatment

Postfabrication N_2O plasma treatment on the ZnO TFTs was carried out in the PECVD system. The process parameters used for the N_2O plasma treatment were as follows: temperature is 300 °C, pressure is 300 mTorr, power is 20 W, and N_2O flow rate is 300 sccm. The duration of the N_2O plasma treatment was varied in the range from 65 to 665 s. The electrical characteristics of the TFTs were measured after each N_2O plasma treatment. XRD, XPS, and PL measurements on the N_2O-treated samples were also carried out.

© 2010 The Japan Society of Applied Physics

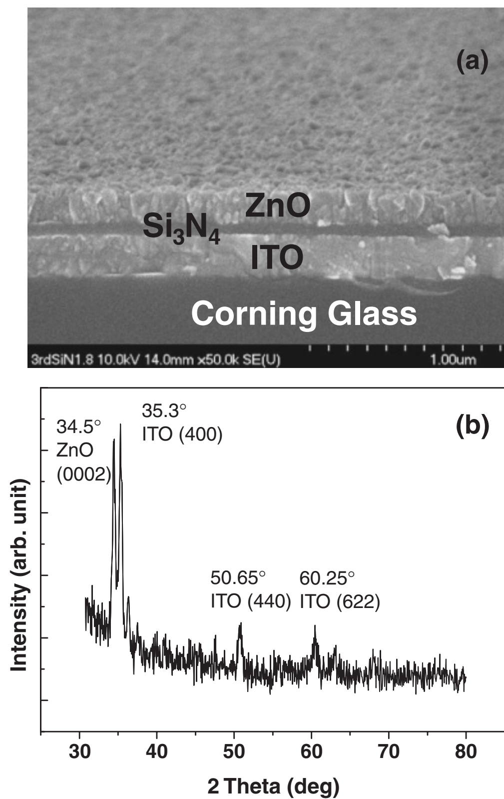

Fig. 2. Morphology and crystalline structure of MOCVD as-grown ZnO films on Si_3N_4/ITO/glass substrates: (a) SEM image. (b) XRD spectrum.

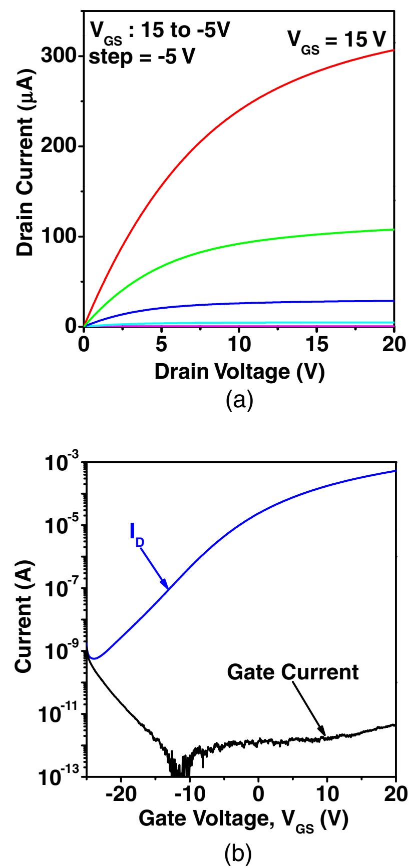

Fig. 3. (Color online) Characteristics of the as-fabricated ZnO TFTs: (a) Output characteristics for V_{GS} varying from 15 to -5 V in steps of -5 V. (b) Transfer characteristics and gate leakage current at V_{DS} = 10 V.

3. Results and Discussion

3.1 Structural properties of as-grown ZnO film

Figure 2 shows the SEM image and XRD spectrum of the ZnO film grown on a Si_3N_4/ITO/glass substrate. The SEM image shows a vertically well-aligned ZnO columnar structure, even though the surface does not appear to be very smooth. The XRD spectrum ($2\theta = 30{-}80°$) shows one strong peak at 34.5°, corresponding to (0002) planes of ZnO, and the other peaks are due to the ITO film.[28] The observation of mainly the (0002) peak from the XRD spectrum indicates that the ZnO film grown on the Si_3N_4 is highly *c*-axis oriented.[29–33] The full width at half maximum (FWHM) of the (0002) ZnO diffraction peak is 0.3404°.

3.2 Characteristics of as-fabricated MOCVD ZnO TFTs

The output characteristics, drain current (I_D) versus drain-to-source voltage (V_{DS}), of the as-fabricated ZnO TFTs are shown in Fig. 3(a). The gate-to-source voltage (V_{GS}) was varied from 15 to -5 V in steps of -5 V. From the output characteristics, it is clear that the ZnO TFTs operate as n-channel devices. The transfer characteristics, I_D versus V_{GS}, of the TFTs measured at $V_{DS} = 10$ V are shown in Fig. 3(b). The characteristics indicate depletion-type operation of the as-fabricated ZnO TFTs. The off-current and on-current were estimated as the minimum and maximum currents, respectively, observed in the transfer characteristics. From Fig. 3(b), it can be seen that the off-current and the on/off current ratio are 0.6 nA and 10^6, respectively. Figure 3(b) also shows the variation of gate current measured as a function of V_{GS} at a V_{DS} of 10 V. It is noteworthy that the off-current is limited by the gate current because gate current is almost the same as drain current in the off-state in Fig. 3(b).

The subthreshold slope (*S*) of TFTs is extracted from its transfer characteristics in the subthreshold regime using the following equation:

$$S = \frac{dV_{GS}}{d \log I_D}. \tag{1}$$

From the subthreshold slope, the equivalent maximum density of states (N_s^{max}) present at the interface between the ZnO channel and the silicon nitride film can be calculated by the following equation:[34]

$$N_s^{max} = \left(\frac{S \log e}{kT/q} - 1\right)\frac{C_i}{q}, \tag{2}$$

where k is the Boltzmann constant, T is the temperature, C_i is the capacitance per unit area of the gate insulator, and q is the unit charge. The estimated S and N_s^{max} of the TFTs are 4.70 V/decade and 2.58×10^{13}/cm^2, respectively. The field-effect mobility (μ_{FE}) and threshold voltage (V_T) of ZnO TFTs operating in the saturation region are estimated from the intercept and slope of the $(I_D)^{0.5}$–V_{GS} curve using the following current equation:[35]

$$I_D = \frac{1}{2} C_i \mu_{FE} \frac{W}{L} (V_{GS} - V_T)^2. \tag{3}$$

The μ_{FE} and V_T of the TFTs are 5 cm^2 V^{-1} s^{-1} and -4 V, respectively. From Fig. 3(b), it can be seen that the drain current is about 24 μA at zero gate voltage, indicating the

© 2010 The Japan Society of Applied Physics

presence of a high concentration of electrons in the as-grown undoped ZnO channel.

It has been previously reported that oxygen vacancies[36–38] and hydrogen[39–45] act as shallow n-type dopants in ZnO materials. Since the zinc source used for ZnO film growth contains hydrogen [$Zn(C_2H_5)_2$], the incorporation of hydrogen into the film may be possible. Thus, the high concentration of electrons in the undoped ZnO film can be attributed to oxygen vacancies and/or residual hydrogen. Jo *et al.*[22] have reported that the hydrogen incorporated into the MOCVD-grown ZnO films during film growth functions as a defect passivator rather than as a shallow dopant. Also, the evolution of hydrogen from the ZnO film during the N_2O plasma treatment may not be possible because Ip *et al.*[46] previously reported that a temperature higher than 500 °C is required for hydrogen to escape from ZnO films. The realization of enhancement-mode MOCVD ZnO TFTs by allowing sufficient oxidation time during ZnO film growth was reported by Jo *et al.*[24] These previous works[22,24] suggest that rather than hydrogen, oxygen vacancies might be the dominant factor responsible for the high concentration of electrons in the MOCVD-grown undoped ZnO films resulting in the depletion-type behavior of ZnO TFTs. However, more experimental work is required to determine the amount of hydrogen in the ZnO film and its exact contribution to the electron concentration. Oxygen vacancies can be reduced by subjecting ZnO films to thermal annealing in oxygen ambient, but this process requires high temperatures typically in the range 450–800 °C.[47,48] Here, we used N_2O plasma treatment at a relatively low temperature to reduce the number of oxygen vacancies. N_2O gas was selected because less energy is required to break the nitrogen–oxygen bond in a N_2O molecule (2.51 eV) than to break the O=O bond in an O_2 molecule (5.12 eV).[49] Thus, it can prevent the ZnO film from becoming conductive via ion bombardment because plasma can be generated at a low RF power.

3.3 Characteristics of N_2O-plasma-treated ZnO TFTs

3.3.1 N_2O plasma treatment for 665 s

The output characteristics of the ZnO TFTs after N_2O plasma treatment for 665 s are shown in Fig. 4(a). These characteristics were measured for V_{GS} ranging from 20 to 0 V in steps of −5 V. Similarly to the as-fabricated devices, the N_2O-treated ZnO TFTs too exhibit n-type device behavior. The transfer characteristics of the N_2O-treated TFTs measured at $V_{DS} = 10$ V are shown in Fig. 4(b). It can be seen from the transfer characteristics that the off-current and on/off current ratio are 0.1 pA and 10^8, respectively. The drain current at zero gate voltage is reduced to 15 pA and V_{on} is −1.5 V. The estimated μ_{FE}, V_T, S, and N_s^{max} are 2.8 cm^2 V^{-1} s^{-1}, 11 V, 0.65 V/decade, and 3.28×10^{12}/cm^2, respectively. These ZnO TFTs operate as enhancement-mode devices, as indicated by the positive value of V_T.

The device parameters of the as-fabricated and N_2O-plasma-treated ZnO TFTs are summarized in Table I. N_2O plasma treatment on the as-fabricated ZnO TFTs changed their device operation from depletion-type to enhancement-type. Compared with the as-fabricated ZnO TFTs, the off-current was about 3 orders of magnitude lower, the subthreshold slope was nearly 7 times lower, and the on/off current ratio was 2 orders of magnitude higher for the N_2O-plasma-treated ZnO TFTs. However, the on-current and μ_{FE} of ZnO TFTs deteriorated after N_2O plasma treatment. The decrease in the on-current value can be attributed to a reduction of carrier concentration in the channel.[50,51] A similar reduction of drain current was previously reported for TFTs using TiO_x[50] and InGaZnO[51] as channel layers when subjected to N_2O plasma treatment to obtain enhancement-mode device operation from depletion-type operation. The decrease in the value of μ_{FE} too can be attributed to a reduction of carrier concentration in the channel layer.[52,53] In order to examine the cause of the improved device performance and enhancement-mode operation of the TFTs,

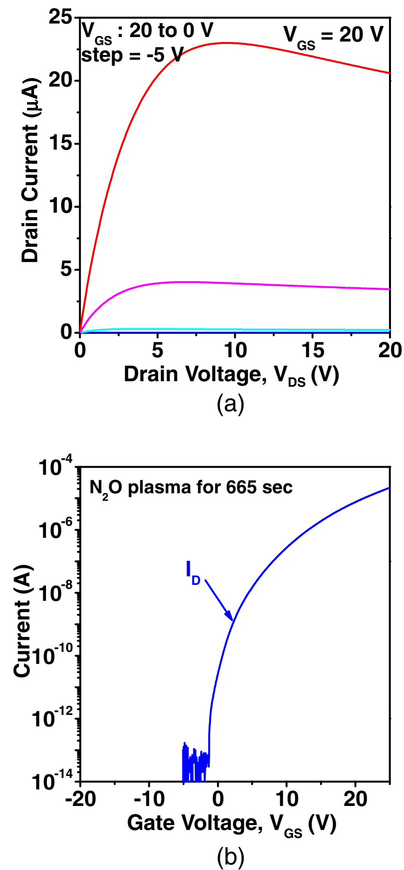

Fig. 4. (Color online) Characteristics of the ZnO TFTs after N_2O treatment for 665 s: (a) Output characteristics for V_{GS} varying from 20 to 0 V in steps of −5 V. (b) Transfer characteristics at $V_{DS} = 10$ V.

Table I. Device parameters of as-fabricated and N_2O-plasma-treated ZnO TFTs.

	As-fabricated	N_2O-plasma-treated
Device operation	*Depletion-mode*	*Enhancement-mode*
Drain current at zero V_{GS}	24 μA	15 pA
V_{on} (V)	−24	−1.5
Off-current	0.6 nA	0.1 pA
On/off current ratio	10^6	10^8
S (V/decade)	4.70	0.65
V_T (V)	−4	11
μ_{FE} (cm^2 V^{-1} s^{-1})	5	2.8
N_s^{max} (/cm^3)	2.58×10^{13}	3.28×10^{12}

© 2010 The Japan Society of Applied Physics

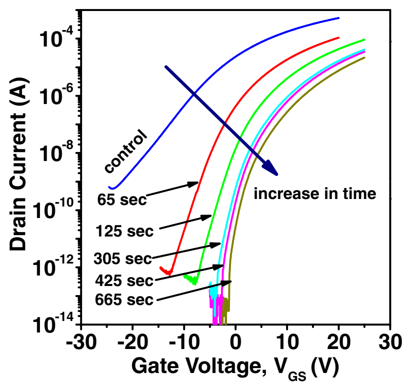

Fig. 5. (Color online) Transfer characteristics of the ZnO TFTs after N_2O treatment for different durations at $V_{DS} = 10$ V.

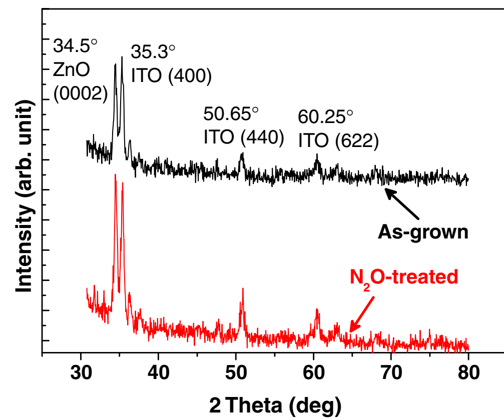

Fig. 6. (Color online) XRD patterns of the as-grown ZnO films before and after N_2O treatment for 665 s.

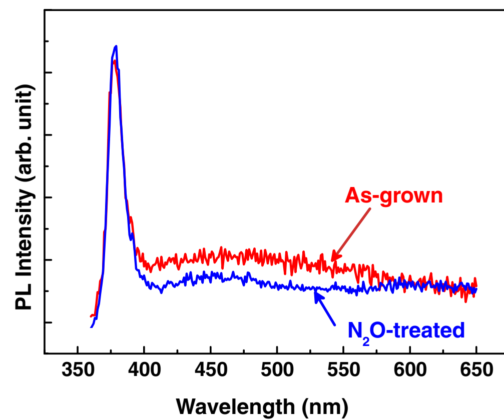

Fig. 7. (Color online) PL spectra of the as-grown ZnO films before and after N_2O treatment for 665 s.

XRD, PL, and XPS measurements were carried out on N_2O-treated and as-grown ZnO samples and the characterization results are described in §3.4.

3.3.2 N_2O plasma treatment for different durations

In order to determine the effect of the duration of N_2O plasma treatment on device characteristics, as-fabricated ZnO TFTs were subjected to N_2O plasma for different times. The transfer characteristics of ZnO TFTs treated for different durations, namely 65, 125, 305, 425, and 665 s are shown in Fig. 5, together with that of the as-fabricated device. It can be seen that the drain current at zero V_{GS} decreases with the increase in N_2O treatment time. The off-current too decreases with increasing N_2O plasma treatment time. The reduction of both the off-current and the drain current at zero V_{GS} can be attributed to a reduction of effective carrier concentration in the ZnO channel layer.

3.4 XRD, PL, and XPS measurements of ZnO films

In order to determine the cause of the enhancement-mode operation as well as the better performance of ZnO TFTs following N_2O plasma treatment, ZnO samples were characterized by the XRD, PL, and XPS methods. Two ZnO samples, namely an as-grown sample and a sample subjected to N_2O plasma treatment for 665 s were used for the measurements; their layer structures were the same as those of the samples used for fabricating TFTs.

3.4.1 XRD and PL

The XRD spectra of the as-grown and N_2O-treated ZnO samples are shown in Fig. 6. The intensity of the (0002) peak of the N_2O-treated sample is stronger than that of the as-grown sample. The FWHM of the (0002) peak for the N_2O-treated sample is 0.3042°, smaller than that for the as-grown sample. The crystalline quality can be evaluated by the FWHM and intensity of the (0002) peak. The higher intensity and narrow FWHM of the (0002) XRD peak for the N_2O-treated sample reveal that this film possesses better crystallinity, which can be attributed to fewer defect states in the film.

Figure 7 shows the room-temperature PL spectra of the as-grown and N_2O-treated ZnO films. From the figure, it is clear that the spectra consist of a strong emission at approximately 380 nm and a weak broad emission band in the visible region (450–550 nm). The peak at approximately 380 nm is the band edge emission, the so-called UV luminescence. The visible emission is due to intrinsic defect states in the ZnO films, such as oxygen vacancies, interstitial zinc, and related defects.[54–56] It is generally accepted that the relative intensity of visible emission in PL reflects the concentration of defects in ZnO. Compared with the as-grown films, the N_2O-treated films exhibit less visible-region luminescence. This result can be attributed to a decrease in the concentration of point defects.

The XRD and PL data indicate that the N_2O-treated sample has better crystallinity and fewer defect states, which may be responsible for the lower values of S and N_s^{max} observed for N_2O-treated ZnO TFTs.

3.4.2 XPS

The samples used for surface analysis were cleaned *in situ* for 5 min using Ar to eliminate the surface contamination before the measurement. The XPS spectra were shifted due to electrostatic charging caused by the use of an insulating glass substrate. Because of this, all spectra were calibrated using C 1s at 284.6 eV as a reference. Figure 8 shows the XPS spectra of O 1s on the surface of as-grown and N_2O-plasma-treated samples. The XPS spectrum of the as-grown sample shows an O 1s peak at 530.59 eV [solid line, Fig. 8(a)] and this energy is assigned to oxygen in the Zn–O bond.[57–61] In the case of the N_2O-treated sample, the O 1s

© 2010 The Japan Society of Applied Physics

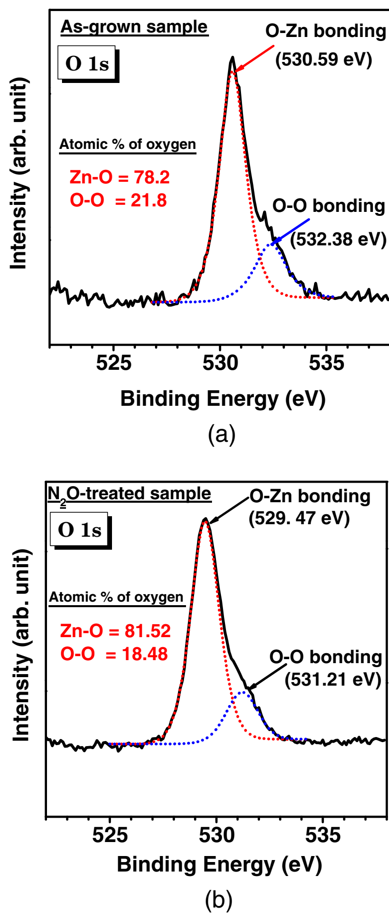

Fig. 8. (Color online) XPS spectra of O 1s on surface of ZnO films. (a) As-grown samples, (b) N_2O-plasma-treated samples.

peak is shifted to a lower binding energy side at 529.47 eV [solid line, Fig. 8(b)]. The movement of the binding energy to a lower value can be due to a decrease in the number of ionized oxygen vacancies in the ZnO film.[57–59,61–63] In general, an ionized oxygen vacancy in a ZnO film donates two electrons to the conduction band, which is mainly responsible for the n-type conductivity of undoped ZnO films. The decrease in electron density due to the reduction of oxygen vacancies moves the Fermi level away from the conduction band, which results in an increase in the work function. This appears to be the reason why the O 1s peak in the XPS spectrum shifted toward a lower binding energy.

In both cases, the O 1s peak can be deconvoluted into two peaks (dotted lines), as shown in Fig. 8. The peak with the lower binding-energy component is assigned to oxygen in the Zn–O bond and the peak with the higher binding-energy component is assigned to oxygen loosely bound on the surface of ZnO.[57–59) From the results of XPS analyses, the normalized atomic percentages of oxygen in the Zn–O bond are 78.2 and 81.52% for the as-grown and N_2O-treated samples, respectively, as shown in Table II. The increased atomic percentage of oxygen in the Zn–O bond in the N_2O-treated sample indicates that the number of ionized oxygen vacancies is decreased in the N_2O-treated sample. Therefore, the enhancement-mode device operation and low off-current of the N_2O-treated ZnO TFTs can be ascribed to the decrease in electron density due to the reduced number of oxygen vacancies in the channel region.

Table II. Atomic percentages of oxygen in Zn–O bond and loosely bound on the surface of as-grown and N_2O-treated ZnO films.

	As-grown (%)	N_2O-treated (%)
Zn–O	78.2	81.52
O–O	21.8	18.48

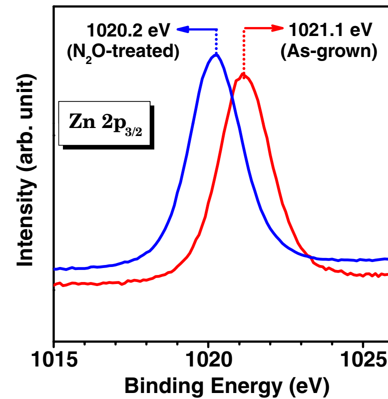

Fig. 9. (Color online) XPS spectra of Zn $2p_{3/2}$ on surface of as-grown and N_2O-plasma-treated ZnO samples.

The Zn $2p_{3/2}$ spectra on the surface of the as-grown and N_2O-plasma-treated ZnO samples are shown in Fig. 9. The as-grown sample shows a Zn peak at 1021.1 eV and this peak corresponds to crystal lattice zinc from ZnO.[57,58,64,65] After the N_2O plasma treatment, the Zn peak moved to a lower-binding-energy position at 1020.2 eV, which shows that an increased number of zinc atoms are bound to oxygen.[64–66] Like in the case of O 1s spectra, the movement of the Zn $2p_{3/2}$ peak too suggests a decrease in the number of oxygen vacancies.

It is known that nitrogen-doped ZnO films show p-type conductivity.[67,68] Therefore, the incorporation of nitrogen from N_2O plasma can also reduce the effective electron concentration of the N_2O-treated ZnO films. But, the XPS spectrum for the N_2O-treated sample did not exhibit any peak related to nitrogen. This suggests that nitrogen had no role in the reduction of electron concentration in the N_2O-treated films.

4. Conclusions

The postfabrication N_2O plasma treatment on the as-fabricated MOCVD ZnO TFTs changed their device operation from depletion-mode to enhancement-mode. N_2O plasma treatment also improved the characteristics of ZnO TFTs in terms of off-current, on/off current ratio, and subthreshold slope. Compared with the as-fabricated ZnO TFTs, the off-current was about 3 orders of magnitude lower, the subthreshold slope was nearly 7 times lower, and the on/off current ratio was 2 orders of magnitude higher for the N_2O-plasma-treated ZnO TFTs. XPS data showed that the number of oxygen vacancies in the N_2O-treated ZnO samples was lower than that in the as-grown samples. The enhancement-mode device operation and improved performance of N_2O-treated ZnO TFTs were therefore attributed to the reduced number of oxygen vacancies in the ZnO

© 2010 The Japan Society of Applied Physics

channel. The number of point defects in the as-grown ZnO film and its crystalline quality were improved following N_2O plasma treatment, as shown by PL and XRD data, respectively.

Acknowledgments

This work was supported by the SEAHERO program under grant no. 07SEAHEROB01-03-01 and the WCU program under grant no. R31-2008-000-10026-0.

1) U. Ozgur, Y. I. Alivov, C. Liu, A. Teke, M. A. Reshchikov, S. Dogan, V. Avrutin, S. J. Cho, and H. Morkoc: J. Appl. Phys. **98** (2005) 041301.
2) X. A. Zhang, J. W. Zhang, W. F. Zhang, D. Wang, Z. Bi, X. M. Bian, and X. Hou: Thin Solid Films **516** (2008) 3305.
3) K. Remashan, D. K. Hwang, S. J. Park, and J. H. Jang: IEEE Trans. Electron Devices **55** (2008) 2736.
4) T. Hirao, M. Furuta, T. Hiramatsu, T. Matsuda, C. Li, H. Furuta, H. Hokari, M. Yoshida, H. Ishii, and M. Kakegawa: IEEE Trans. Electron Devices **55** (2008) 3136.
5) E. M. C. Fortunato, P. M. C. Barquinha, A. C. M. B. G. Pimentel, A. M. F. Gonçalves, A. J. S. Marques, R. F. P. Martins, and L. M. N. Pereira: Appl. Phys. Lett. **85** (2004) 2541.
6) R. Martins, P. Barquinha, I. Ferreira, L. Pereira, G. Gonçalves, and E. Fortunato: J. Appl. Phys. **101** (2007) 044505.
7) Dhananjay and S. B. Krupanidhi: J. Appl. Phys. **101** (2007) 123717.
8) P. F. Carcia, R. S. McLean, and M. H. Reilly: Appl. Phys. Lett. **88** (2006) 123509.
9) R. B. M. Cross, M. M. D. Souza, S. C. Deane, and N. D. Young: IEEE Trans. Electron Devices **55** (2008) 1109.
10) P. F. Carcia, R. S. McLean, M. H. Reilly, M. K. Crawford, and E. N. Blanchard: J. Appl. Phys. **102** (2007) 074512.
11) P. K. Shin, Y. Aya, T. Ikegami, and K. Ebihara: Thin Solid Films **516** (2008) 3767.
12) J. Siddiqui, E. Cagin, D. Chen, and J. D. Phillips: Appl. Phys. Lett. **88** (2006) 212903.
13) I. D. Kim, Y. W. Choi, and H. L. Tuller: Appl. Phys. Lett. **87** (2005) 043509.
14) B. Bayraktaroglu, K. Leedy, and R. Neidhard: IEEE Electron Device Lett. **29** (2008) 1024.
15) S. Masuda, K. Kitamura, Y. Okumura, S. Miyatake, H. Tabata, and T. Kawai: J. Appl. Phys. **93** (2003) 1624.
16) N. Huby, S. Ferrari, E. Guziewicz, M. Godlewski, and V. Osinniy: Appl. Phys. Lett. **92** (2008) 023502.
17) D. H. Levy, D. Freeman, S. F. Nelson, P. J. C. Corvan, and L. M. Irving: Appl. Phys. Lett. **92** (2008) 192101.
18) S. H. K. Park, C. S. Hwang, H. Y. Jeong, H. Y. Chu, and K. I. Cho: Electrochem. Solid-State Lett. **11** (2008) H10.
19) J. Sun, D. A. Mourey, D. Zhao, S. K. Park, S. F. Nelson, D. H. D. Freeman, P. C. Corvan, L. Tutt, and T. N. Jackson: IEEE Electron Device Lett. **29** (2008) 721.
20) S. Kwon, S. Bang, S. Lee, S. Jeon, W. Jeong, H. Kim, S. C. Gong, H. J. Chang, H. Park, and H. Jeon: Semicond. Sci. Technol. **24** (2009) 035015.
21) S. H. K. Park, C. S. Hwang, M. Ryu, S. Yang, C. Byun, J. Shin, J. I. Lee, K. Lee, M. S. Oh, and S. Im: Adv. Mater. **21** (2009) 678.
22) J. Jo, O. Seo, E. Jeong, H. Seo, B. Lee, and Y. I. Choi: Jpn. J. Appl. Phys. **46** (2007) 2493.
23) J. Zhu, H. Chen, G. Saraf, Z. Duan, Y. Lu, and S. T. Hsu: J. Electron. Mater. **37** (2008) 1237.
24) J. Jo, O. Seo, H. Choi, and B. Lee: Appl. Phys. Express **1** (2008) 041202.
25) G. B. Stringfellow: *Organometallic Vapor-Phase Epitaxy: Theory and Practice* (Academic Press, New York, 1998) 2nd ed., p. 4.
26) C. W. Chen, T. C. Chang, P. T. Liu, H. Y. Lu, K. C. Wang, C. S. Huang, C. C. Ling, and T. Y. Tseng: IEEE Electron Device Lett. **26** (2005) 731.
27) J. W. Park, D. Lee, H. Kwon, and S. Yoo: IEEE Electron Device Lett. **30** (2009) 362.
28) M. H. Yang, J. C. Wen, K. L. Chen, S. Y. Chean, and M. S. Leu: Thin Solid Films **484** (2005) 39.
29) K. Kim, K. C. Park, and D. Y. Ma: J. Appl. Phys. **81** (1997) 7764.
30) K. S. Kim, H. W. Kim, and C. M. Lee: Mater. Sci. Eng. B **98** (2003) 135.
31) Y. Zhang, G. Du, B. Liu, H. C. Zhu, T. Yang, W. Li, D. Liu, and S. Yang: J. Cryst. Growth **262** (2004) 456.
32) R. Menon, K. Sreenivas, and V. Gupta: J. Appl. Phys. **103** (2008) 094903.
33) J. H. Kwon, J. H. Seo, S. I. Shin, and B. K. Ju: J. Phys. D **42** (2009) 065105.
34) J. Kanicki and S. Martin: in *Thin-Film Transistors*, ed. C. R. Kagan and P. Andry (Marcel Dekker, New York, 2003) p. 87.
35) H. H. Hsieh and C. C. Wu: Appl. Phys. Lett. **89** (2006) 041109.
36) Y. Ma, G. T. Du, T. P. Yang, D. L. Qiu, X. Zhang, H. J. Yang, Y. T. Zhang, B. J. Zhao, X. T. Yang, and D. L. Liu: J. Cryst. Growth **255** (2003) 303.
37) K. Vanheusden, C. H. Seager, W. L. Warren, D. R. Tallant, and J. A. Voigt: Appl. Phys. Lett. **68** (1996) 403.
38) A. Poppl and G. Volkel: Phys. Status Solidi A **125** (1991) 571.
39) C. A. Wolden, T. Barnes, J. B. Baxter, and E. S. Aydil: J. Appl. Phys. **97** (2005) 043522.
40) C. G. Van de Walle: Phys. Rev. Lett. **85** (2000) 1012.
41) S. F. J. Cox, E. A. Davis, S. P. Cottrell, P. J. C. King, J. S. Lord, J. M. Gil, H. V. Alberto, R. C. Vilao, J. P. Duarte, N. A. de Campos, A. Weidinger, R. L. Lichti, and S. J. C. Irvine: Phys. Rev. Lett. **86** (2001) 2601.
42) D. M. Hofmann, A. Hofstaetter, F. Leiter, H. Zhou, F. Henecker, B. K. Meyer, S. B. Orlinskii, J. Schmidt, and P. G. Baranov: Phys. Rev. Lett. **88** (2002) 045504.
43) E. V. Monakhov, J. S. Christensen, K. Maknys, B. G. Svensson, and A. Yu. Kuznetsov: Appl. Phys. Lett. **87** (2005) 191910.
44) J. B. You, X. W. Zhang, P. F. Cai, J. J. Dong, Y. Gao, Z. G. Yin, N. F. Chen, R. Z. Wang, and H. Yan: Appl. Phys. Lett. **94** (2009) 262105.
45) Y. J. Li, T. C. Kaspar, T. C. Droubay, Z. Zhu, V. Shutthanandan, P. Nachimuthu, and S. A. Chambers: Appl. Phys. Lett. **92** (2008) 152105.
46) K. Ip, M. E. Overberg, Y. W. Heo, D. P. Norton, S. J. Pearton, C. E. Stutz, B. Luo, F. Ren, D. C. Look, and J. M. Zavada: Appl. Phys. Lett. **82** (2003) 385.
47) D. Redinger and V. Subramanian: IEEE Trans. Electron Devices **54** (2007) 1301.
48) R. L. Hoffman, N. Norris, and J. F. Wager: Appl. Phys. Lett. **82** (2003) 733.
49) W. S. Lau, P. W. Qian, N. P. Sandler, K. A. McKinley, and P. K. Chu: Jpn. J. Appl. Phys. **36** (1997) 661.
50) J. W. Park, D. Lee, H. Kwon, and S. Yoo: IEEE Electron Device Lett. **30** (2009) 362.
51) J. Park, S. Kim, C. Kim, S. Kim, I. Song, H. Yin, K. K. Kim, S. Lee, K. Hong, J. Lee, J. Jung, E. Lee, K. W. Kwon, and Y. Park: Appl. Phys. Lett. **93** (2008) 053505.
52) S. I. Kim, C. J. Kim, J. C. Park, I. Song, S. W. Kim, H. Yin, E. Lee, J. C. Lee, and Y. Park: IEDM Tech. Dig., 2008, p. 73.
53) P. F. Carcia, R. S. McLean, M. H. Reilly, and G. Nunes: Appl. Phys. Lett. **82** (2003) 1117.
54) Y. J. Lin and C. L. Tsai: J. Appl. Phys. **100** (2006) 113721.
55) B. Lin, Z. Fu, Y. Jia, and G. Liao: J. Electrochem. Soc. **148** (2001) G110.
56) L. Zhao, J. Lian, Y. Liu, and Q. Jiang: Appl. Surf. Sci. **252** (2006) 8451.
57) Z. G. Wang, X. T. Zu, S. Zhu, and L. M. Wang: Physica E **35** (2006) 199.
58) M. Chen, X. Wang, Y. H. Yu, Z. L. Pei, X. D. Bai, C. Sun, R. F. Huang, and L. S. Wen: Appl. Surf. Sci. **158** (2000) 134.
59) T. Szorenyi, L. D. Laude, I. Bertoti, Z. Kantor, and Z. G. Vszky: J. Appl. Phys. **78** (1995) 6211.
60) L. Zhang, Z. Chen, Y. Tang, and Z. Jia: Thin Solid Films **492** (2005) 24.
61) S. H. Kim, Y. K. Moon, D. Y. Moon, M. S. Hong, Y. J. Jeon, J. W. Park, and C. H. Jeong: J. Korean Phys. Soc. **49** (2006) 1256.
62) C. C. Lin, H. P. Chen, H. C. Liao, and S. Y. Chen: Appl. Phys. Lett. **86** (2005) 183103.
63) J. C. C. Fan and J. B. Goodenough: J. Appl. Phys. **48** (1977) 3524.
64) Y. Zhang, G. Du, X. Wang, W. Li, X. Yang, Y. Ma, B. Zhao, H. Yang, D. Liu, and S. Yang: J. Cryst. Growth **252** (2003) 180.
65) H. Li, H. Liu, J. Wang, S. Yao, X. Cheng, and R. I. Boughton: Mater. Lett. **58** (2004) 3630.
66) G. E. B. Core, G. Cabello, A. H. Klahn, R. D. Rio, and R. H. Hill: J. Non-Cryst. Solids **352** (2006) 4088.
67) B. Yao, D. Z. Shen, Z. Z. Zhang, X. H. Wang, Z. P. Wei, B. H. Li, Y. M. Lv, X. W. Fan, L. X. Guan, G. Z. Xing, C. X. Cong, and Y. P. Xie: J. Appl. Phys. **99** (2006) 123510.
68) S. Gangil, A. Nakamura, M. Shimomura, and J. Temmoyo: Jpn. J. Appl. Phys. **46** (2007) L549.

© 2010 The Japan Society of Applied Physics